Hydrol. Earth Syst. Sci. Discuss., 8, 2175–2205, 2011
www.hydrol-earth-syst-sci-discuss.net/8/2175/2011/
doi:10.5194/hessd-8-2175-2011

Hydrology and Earth System Sciences Discussions

Quantifying spatial and temporal discharge dynamics of an event in a first order stream, using Distributed Temperature Sensing

M. C. Westhoff[1], **T. A. Bogaard**[1,2], **and H. H. G. Savenije**[1]

[1]Water Resources Section, Faculty of Civil Engineering and Geosciences, Delft University of Technology, P.O. Box 5048, 2600 GA Delft, The Netherlands
[2]Centre de Recherche Public Gabriel Lippmann, Department Environment and Agro-Biotechnologies, 4422 Belvaux, Grand-Duchy of Luxembourg

Received: 25 February 2011 – Accepted: 25 February 2011 – Published: 1 March 2011

Correspondence to: M. C. Westhoff (m.c.westhoff@tudelft.nl)

Published by Copernicus Publications on behalf of the European Geosciences Union.

Abstract

Understanding spatial distribution of discharge can be important for water quality and quantity modeling. Non-steady flood waves can influence small headwater streams significantly, particularly as a result of short high intensity summer rainstorms. The aim of this paper is to quantify the spatial and temporal dynamics of stream flow in a headwater catchment during a summer rainstorm. These dynamics include gains and losses of stream water, the effect of bypasses that become active and hyporheic exchange fluxes that may vary over time as a function of discharge. We use an advection-dispersion model coupled with an energy balance model to simulate in-stream water temperature, which we confront with high resolution temperature observations obtained with Distributed Temperature Sensing. This model was used as a learning tool to stepwise unravel the complex puzzle of in-stream processes subject to varying discharge. Hypotheses were tested and rejected, which led to more insight in spatial and temporal dynamics in discharge and hyporheic exchange processes. We showed that infiltration losses increase during a rain event, while gains of water remained constant over time. We conclude that, eventually, part of the stream water bypassed the main channel during peak discharge. It also seems that hyporheic exchange varies with varying discharge in the first 250 of the stream; while further downstream it remains constant. Because we relied on solar radiation as the main energy input, we were only able to apply this method during a small event and low flow. However, when additional (artificial) energy is available, the presented method is also applicable in larger streams, or during higher flow conditions.

1 Introduction

Understanding discharge generation processes in headwater catchments is crucial for water quality and quantity modeling (Bonell, 1998). However, it is often difficult to differentiate between different runoff generation processes. A classical way to do this

HESSD
8, 2175–2205, 2011

is by hydrograph separation techniques using end-member mixing analysis approach (Sklash and Farvolden, 1979). This technique can be useful in differentiating between different source areas or between event and pre-event water (Uhlenbrook and Hoeg, 2003). However, spatial resolution is often low, fluxes are lumped and uncertainties can be high.

Understanding spatial distribution of discharge can be important since non-steady flood waves can influence small headwater streams significantly, particularly as a result of short high intensity summer rainstorms. During such events, discharge can more than double, and side channels can become active. Also subsurface storm flow may occur, although a certain storage threshold in the hillslope has to be passed before this mechanism becomes active (e.g. Tromp-van Meerveld and McDonnell, 2006).

To observe the spatial and temporal distribution of lateral inflows, several researches excavated trenches (Woods and Rowe, 1996; Weiler et al., 1998; Uchida et al., 2005; Retter et al., 2006; Gomi et al., 2008; Tromp-van Meerveld et al., 2008). Although these were able to give spatial and temporal flow information, installation of trenches is destructive and limited in size (2–60 m).

Another approach was presented by Ragan (1968). He monitored all incoming water fluxes in a 190 m long stretch, including the change of in-stream storage. He added one term to close the water balance, which he concluded to be subsurface stormflow. Although he is one of few who gained insights in temporal and spatial dynamics of lateral inflow without the use of trenches or 3-D groundwater-surface water models, he did not include infiltration losses of stream water or hyporheic exchange in his analysis while also the location of the calibrated subsurface stormflow was unknown.

Stream water losses (or downwelling fluxes) are difficult to quantify, since it does not influence stream water quality directly. To determine these fluxes, some researchers observed vertical subsurface temperature profiles, which, when coupled with a vertical advection-dispersion model gave flow rates and directions (Stallman, 1965; Lapham, 1989; Taniguchi and Sharma, 1990; Silliman et al., 1995; Constantz and Thomas, 1996; Constantz, 1998; Constantz et al., 2003; Becker et al., 2004; Niswonger et al.,

HESSD
8, 2175–2205, 2011

2005; Blasch et al., 2007). However, these profiles were point measurements along the stream, obtained during steady state discharge conditions.

Moreover, hyporheic exchange fluxes may change with varying discharge. This triggered research on seasonal changes in hyporheic exchange, determined from head differences in a vertical profile using piezometer nests (Harvey and Bencala, 1993; Wroblicky et al., 1998; Bartolino, 2003). In addition, on the timescale of one flood wave, coupled 3-D groundwater-surface water models were developed (Lal, 2001; Habel and Bagtzoglou, 2005; Boano et al., 2007; Ha et al., 2008). However, these deterministic models require an accurate description of hydraulic conductivities and bedforms while such data are often not available. To overcome this problem, hyporheic exchange has been quantified using in-stream tracer tests. Most studies linking hyporheic exchange with discharge did their tracer tests during different discharge regimes (Legrand-Marcq and Laudelout, 1985; Harvey et al., 1996; Morrice et al., 1997; Zarnetske et al., 2007; Schmid, 2008; Schmid et al., 2010), different morphological states (Hart et al., 1999; Harvey et al., 2003) or between different streams (D'angelo et al., 1993; Morrice et al., 1997; Schmid et al., 2010), but always during steady state flow conditions and not during a complete rainstorm.

The aim of this paper is to quantify the spatial and temporal dynamics of stream flow in a headwater catchment during a summer rainstorm. These dynamics include gains and losses of stream water, the effect of bypasses that become active and hyporheic exchange fluxes that may vary over time as a function of dicharge. In a previous study we showed the relation between hydraulics, in-stream temperature and hyporheic exchange in a first order stream during steady state discharge conditions (Westhoff et al., 2011). In this paper we focus on the dynamic effects that occur during and after a small intensive summer rainstorm. We use an advection-dispersion model coupled with an energy balance model to simulate in-stream water temperature, which we confront with high resolution temperature observations obtained with Distributed Temperature Sensing (DTS). Together with upstream and downstream discharge observations, we were able to locate and estimate the dynamics of hyporheic exchange, lateral inflows and

HESSD
8, 2175–2205, 2011

bypasses. We used the method as a learning tool in which we stepwise unravel the complex interactions and dynamics in discharge.

2 Site description and measurements

2.1 Site description

This research took place in a 565 m long branch of the Maisbich: a first order stream in central Luxembourg (49°53′ N and 6°02′ E). The investigated branch drains an area of 0.34 km^2. The stream has an average slope of 18%, with on both sides steep forested hillslopes (Fig. 1).

The schist bedrock is covered by a few meter thick layer of fractured rock, with varying clay content. On top of this layer, a layer of fine sediments developed which is <1 m thick in the riparian zone and on the hillslopes. On the plateau, this layer is a couple of meters thick. Most of the water drains from the plateau. The stream originates in a small depression at the transition between hillslope and plateau. Around the stream, colluvial sediments and a thin soil layer, cover the schist. The stream scoured the soil layer, creating at many places steep banks of 0.2–1 m high. The streambed is rough with many in-stream rock clasts. Summer storm flows are characterized by a double peak: the first peak is mainly caused by "rain on water" and rain on saturated riparian land (saturation overland flow), while the second peak is assumed to be subsurface storm flow (Fig. 2).

Along the stream, 4 distinct lateral, partly submerged inflows are present at 104, 178, 350 and 414 m from the upstream V-notch wier, respectively. These inflows generally are cracks in the underlying bedrock from where water seeps to the stream. Two smaller inflows enter the stream at 383 and 393 m, but they are <5% of the discharge directly downstream of the inflow, and too small to monitor. During the studied period (22 and 23 June 2008), two areas of stream water loss were identified: one area between 60 and 77 m where ~90% of water infiltrates into the subsurface and a smaller

HESSD
8, 2175–2205, 2011

one between 233 and 247 m where ~45% of the water infiltrates. In-stream salt injection tests during previous field campaigns demonstrated, that at least part of the water that infiltrates between 60 and 77 m, returns to the stream at 104 m (data not shown). A previous study by Westhoff et al. (2011) showed that at many places along the stream small scale hyporheic exchange is present.

2.2 Measurements

Two V-notch weirs are present at the upstream and downstream end of the studied stream reach. They have been equipped with pressure loggers (Keller DCX22), monitoring water levels at 10 min intervals. During the studied period, the pre-event discharge was 0.44 and 0.65 $l\,s^{-1}$ for the upstream and downstream V-notch weir, respectively. Peak discharge was 1.9 and 1.8 $l\,s^{-1}$ (Fig. 2).

Along the entire stream, temperature was measured with a DTS system (Halo, Sensornet, UK). The system gives an integrated temperature for each 2 m along a fiber optic cable which is averaged over 3 min. The precision, using these settings, is ~0.1 °C. Comparison with independent temperature loggers (TidbiT v2 Temp logger, HOBO, USA) at 12, 176 and 347 m gave a Root Mean Square Error (RMSE) of 0.27 °C (for a more detailed description about DTS see, Selker et al., 2006a,b; Tyler et al., 2009).

The water temperature of each of the 4 distinct sources was measured with independent temperature loggers (TidbiT v2 Temp logger, HOBO, USA) at a 6 minute interval. At the 3 most upstream inflows, also the stream water temperature just upstream and downstream of the inflow was measured with the TidbiT temperature loggers.

In the meadow just uphill of the upper V-notch weir, a HOBO weather station was installed, measuring incoming solar radiation, air temperature, air pressure, wind speed and wind direction. Relative humidity was measured in Ettelbruck (~6 km from the site) by the Administration des Services Techniques de l'Agriculture (http://www.asta.etat.lu), with a temporal resolution of 10 min.

HESSD
8, 2175–2205, 2011

3 Methods

3.1 Previous work and model description

This study builds on previous work by Westhoff et al. (2007, 2010, 2011). In this section we only give a short description of this work. For further details, the reader is referred to the original studies.

The used model consists of three coupled models: a hydraulic routing model, a transport model for temperature and an energy balance model. The routing model is based on the Saint Venant equation (Stelling and Duinmeijer, 2003) and is used to determine the spatial and temporal varying discharge, cross-sectional area, width and wetted perimeter of the stream, which are all input variables for the transport and energy balance model. The relative contributions of the four distinct lateral inflows are determined by a simple mass balance using the observed temperatures upstream and downstream of the lateral inflow and of the inflow itself (Westhoff et al., 2010). The infiltration losses and the two small inflows are estimated by comparing the observed upstream discharge plus all inflows and losses with the observed downstream discharge.

The transport model is based on the advection-dispersion equation with 2 transient storage zones. One transient storage zone represents heat exchange with in-stream rock clasts, which Westhoff et al. (2010) found to be an important mechanism in this stream. The heat exchange with the in-stream rock clasts is assumed to be instantaneous, meaning that the rock clasts always have the same temperature as the surrounding water.

The second transient storage zone represents the hyporheic zone (Westhoff et al., 2011). These zones are assumed to be well mixed reservoirs and situated in the subsurface below the stream, where they also exchange heat with the deeper soil. No lateral hyporheic flowpaths have been taken into account. The exchange coefficient (α) and volume of the hyporheic zone ($A_s dx$) were calibrated by Westhoff et al. (2011) for steady state summer baseflow. Flow conditions during their study were similar to the

HESSD
8, 2175–2205, 2011

pre-event conditions of this study. The hyporheic zone is assumed to be located under the stream and has the same width as the wetted perimeter.

The energy balance model is a sink/source term in the transport model, taking the solar radiation, longwave radiation, latent heat, sensible heat and riverbed conduction into account, and is determined for each time step (Westhoff et al., 2007). Westhoff et al. (2011) made a few changes to this model: The riverbed conduction is determined up to a depth of 1 m below the stream and the latent and sensible heat equations are taken from Monteith (1981). This is because we observed relative humidities of up to 100% during this study, while the Bowen ratio used in Westhoff et al. (2007) is not suitable for such high relative humidities.

The governing equations of the transport model are:

$$\frac{\partial A_w}{\partial t} + \frac{\partial Q}{\partial x} = q_L + RW_R \tag{1}$$

$$\rho_b c_b \frac{\partial A_b T_w}{\partial t} + \rho_w c_w \frac{\partial Q T_w}{\partial x} + \rho_w c_w \frac{\partial}{\partial x}\left(-A_w D \frac{\partial T_w}{\partial x}\right) = \rho_w c_w (q_L T_L + RW_R T_R) + \rho_w c_w \alpha A_w (T_{hz} - T_w) + W_b \Phi_{atm} + P_b \Phi_{bed} \tag{2}$$

$$\frac{\partial T_s}{\partial t} = -K_s \frac{\partial^2 T_s}{\partial z^2} + \alpha \frac{A_w}{A_{hz}} (T_w - T_{hz}) - \frac{\Phi_{bed}}{c_b \rho_b dz} \tag{3}$$

where Q, A and T are the discharge [$m^3 s^{-1}$], cross-sectional area [m^2] and temperature [°C]. R is the precipitation [$m s^{-1}$], W_R the width at which the precipitation turns immediately into runoff [m] and T_R is the temperature of the precipitation [°C]. q_L is the lateral inflow per unit stream length [$m^2 s^{-1}$], ρ and c are the density [$kg m^{-3}$] and heat capacity [$J kg^{-1} °C^{-1}$], D is the longitudinal dispersion coefficient [$m^2 s^{-1}$], α is the hyporheic exchange coefficient [s^{-1}], W_b and P_b are the width [m] and the wetted perimeter [m]. Φ_{atm} and Φ_{bed} are the net energy exchange [$W m^{-2}$] through the water-air interface

HESSD
8, 2175–2205, 2011

and water-streambed interface, respectively and K_s is the thermal diffusivity of the subsurface [$m^2\ s^{-1}$], while t, x and z are time [s], distance along the stream [m] and depth below the stream [m]. The subscripts w, L, s and hz stand for water, lateral inflow, subsurface and hyporheic zone, while b stands for the bulk of stream water and in-stream rock clasts.

In Eq. (3), the second term on the right hand side is only taken into account for the locations (longitudinal as well as vertical) where hyporheic exchange was identified. The third term describes the heat exchange between the subsurface and the stream and is therefore only applied at the top layer of the subsurface.

This model was calibrated for a 2 day period in July 2009, during steady state discharge conditions with the aim of assessing hyporheic exchange (Westhoff et al., 2011). For this study, we first validated the model for a 2 day period prior to a rainfall event at 22 June 2008 20:40, during which the discharge was steady.

3.2 Stepwise improvement of dynamic discharge simulations

In this study, we follow a downward approach in which we stepwise improve the model (Klemeš, 1983; Jothityangkoon et al., 2001; Sivapalan et al., 2003). This means that we first model a simple case, and based on the results, we stepwise increase model complexity and develop and test new hypotheses to improve the model results. We combine this with a multi-objective model evaluation (Fenicia et al., 2008). The objective functions are (1) the Root Mean Square Error of the downstream discharge ($RMSE_Q$), (2) the Root Mean Square Error of the in-stream temperature ($RMSE_T$) and (3) the Root Mean Square Error of the relative contribution of the second lateral inflow at 178 m ($RMSE_L$).

For calibration, we split the observed hydrograph in two parts because different processes are responsible for the discharge peaks: the first peak is mainly caused by rain on water, while the second peak is assumed to be caused by subsurface storm flow.

HESSD
8, 2175–2205, 2011

3.2.1 First discharge peak

In a first step we only focus on the first discharge peak (between 22 June 2008 20:40 and 23 June 2008 01:00). Here we calibrated 3 parameters. These parameters are: (1) the losses of water which we describe as a function of discharge, (2) the area where saturation overland flow takes place (W_R): this is the stream itself and its near surroundings and (3) the temperature of the rain water (T_R). The first two influences both downstream discharge and in-stream temperature, while the third parameter only influences in-stream temperature.

3.2.2 Second discharge peak

During the second step of the calibration we focus on different processes that occur during the second discharge peak, which we assume is subsurface storm flow orriginating from the area upstream of the upstream V-notch weir. We first extend the simulation period of the first step with 9 h until 23 June 2008 10:00 to cover the second discharge peak, without changing any parameter. In this run we found a couple of mismatches between observed and simulated discharge and temperature. For reasons of clarity we treat these temperature and discharge mismatches separately, although we recognize that discharge influences temperature as well.

In-stream temperature

To improve the simulated temperature, we investigated the effect of constant and variable hyporheic exchange parameters (i.e. the flux between the stream and hyporheic zone, and volume of the hyporheic zone). This results in 4 different alternatives:

1. $Q_{hyp} = \alpha A_w dx$ and $V_{hz} = A_{hz} dx = P_b z_{hz} dx$, where z_{hz} is the thickness of the hyporheic zone, and is assumed to be constant in time. For the exchange flux we

HESSD
8, 2175–2205, 2011

used the widely used expression from Runkel (1998). For the volume of the hyporheic zone we assumed that the thickness would remain the same, and V_{hz} depends linearly on the wetted perimeter of the stream.

2. Both the Q_{hyp} and V_{hz} are constant over time and keep the pre-event values.
3. $Q_{hyp} = \alpha A_w dx$ and V_{hz} is constant over time.
4. Q_{hyp} is constant over time and $V_{hz} = P_b z_{hz} dx$.

Discharge

The calibrated run of the first discharge peak was used for the second peak. This simulation resulted in a difference between simulated and observed downstream discharge for the second peak. In this step we took the difference between observed and simulated downstream discharge, and added this as a lateral inflow at distance x_i. By changing the position of this new lateral inflow, we tested 3 different hypotheses on where this water came from.

1. As a diffuse source between 250 and 350 m. The reason for this is that when this new water is cooler than the stream water (as a first estimate we took the temperature of the third lateral inflow for the temperature of this new inflow), it would cool down the stream water, which would result in a better fit.
2. As extra water from the second lateral inflow point at 178 m. Reason for this is that when the stream discharge is higher, the water would not heat up as rapidly. The reason for adding this new water at an already existing source is that preferential flowpaths already direct water to this point. Extra subsurface storm flow would then easily directed to the same place.

HESSD
8, 2175–2205, 2011

3. As a new source at 117 m. During high (winter) flows, we have observed that part of the stream water bypassed the channel between ~80 and 117 m. Here we test if this also happens during this summer rain storm.

4 Results

Validation of the model as calibrated by Westhoff et al. (2011) was done for the period 21 June 2008 00:00 until 22 June 2008 20:40, which was just before the start of the storm event. The validation run had a $RMSE_T$ of 0.51 °C (for comparison: the $RMSE_T$ of the calibrated model was 0.66 °C for the same time span at 1 and 2 July 2009). The difference in the $RMSE_T$ was mainly caused by the fact that during the calibration period the fiber optic cable was not submerged at a few distinct places. During the validation the simulated temperature downstream of 420 m was about 1 °C too high during the night.

4.1 First discharge peak

The first discharge peak was calibrated by varying the infiltration losses ($q_L < 0$), the width accounting for "rain on water" (W_R) and the temperature of the rain (T_R). Keeping the losses constant over time and W_R the same as the stream width W_b, resulted in a simulated downstream peak discharge arriving 50 min too late (line *a* in Fig. 3). Therefore we made the losses dependent on discharge (line *b* in Fig. 3): between 233 and 247 m the loss was set to be 45% of the discharge at 232 m. Between 60 and 77 m, the loss was set to 95% during pre-event discharge ($0.4\,l\,s^{-1}$) and 88% during peak discharge ($1.9\,l\,s^{-1}$). To be able to simulate the observed downstream discharge peak properly, we had to change W_R to 1.7 m for the entire stream to account for the additional saturated overland flow. After this refinement we obtained a $RMSE_Q$ of $0.11\,l\,s^{-1}$ (line *c* in Fig. 3). Good temperature simulations were obtained when T_R

HESSD
8, 2175–2205, 2011

was taken 2.4 °C lower than T_{air}, which can be seen as a correction for the wet bulb temperature. This resulted in a $RMSE_T$ of 0.34 °C (Fig. 4a).

4.2 Second discharge peak

Extending the simulation period until the second discharge peak, while keeping the same parameters as during the first discharge peak, resulted in a too low downstream discharge between 03:00 and 10:00 h (Fig. 5). During the same period, the temperature between 250 and 350 m and downstream of 420 m was also too high (Fig. 4b). Here, we treat both discrepancies separately.

In-stream temperature

Although we recognize that discharge influences in-stream temperature as well, we focus first on the influence of different hyporheic exchange scenarios. The 4 different scenarios tested ($Q_{hyp} = \alpha A_w dx$ and $V_{hz} = P_b z_{hz} dx$; Q_{hyp} and V_{hz} are constant over time; $Q_{hyp} = \alpha A_w dx$ and V_{hz} is constant over time; and Q_{hyp} is constant over time and $V_{hz} = P_b z_{hz} dx$), gave different results for different sections in the stream. In Fig. 6a the $RMSE_T$ is shown for the time series between 01:00 and 10:00 h for each observation point (a moving average over 3 points was plotted to get slightly smoother lines). Until 250 m the temperature was best simulated when both the hyporheic flux and the volume of the hyporheic zone were taken variable over time, while downstream of 250 m best results were obtained when both were constant over time. From Fig. 6a, it is also seen that when only V_{hz} is variable while Q_{hyp} is constant, results hardly differ from the case where both are constant over time. The difference between a constant and variable V_{hz} is slightly larger when Q_{hyp} is variable.

HESSD
8, 2175–2205, 2011

Discharge

During the second peak, the simulated downstream discharge is too low between 03:00 and 10:00 h: apparently there is some lateral inflow, which we did not encount for (Fig. 5). The difference between the two hydrographs (shaded area in Fig. 5) has been added to the stream at different locations x_i, while we used the $RMSE_T$ and $RMSE_L$ to test the effect of the different locations (the $RMSE_Q$ are equal for each scenario, because the same amount of water was added for each scenario). As a reference case, we used a hyporheic exchange scenario during which Q_{hyp} and V_{hz} are variable between 0 and 250 m while downstream of 250 m they are constant over time. Because the temperature downstream of 420 m was also too high during the validation, we only focus on the area upstream of 420 m.

Between 117 and 260 m, the $RMSE_T$ is the lowest when the new source is added at 117 m. Between 260 and 320 m best results were obtained when the new source was added at 178 m, while downstream of 320 m the diffuse source added between 250 and 350 m gave best results (Fig. 6b). Comparing the different scenarios with the observed relative contribution of the second source, shows the best results when water is added at 117 m, (Fig. 7, $RMSE_L$ is 4.3% for the time series between 01:00 and 10:00 h), with slightly poorer performance for the diffuse source ($RMSE_L$ is 5.8%). Note that the latter does not effect the seconds source compared to the reference simulation, since the new source was added downstream of this point. The scenario where the source was added as extra water at the second source totally mismatches the observations ($RMSE_L$ is 18.2%), indicating that this hypothesis should be rejected.

HESSD
8, 2175–2205, 2011

5 Discussion

5.1 Reality check

The presented method combines 2 sources of information: discharge observations and temperature observations. By combining these, we were able to investigate the spatial and temporal distribution of discharge along the whole length of the stream. In our approach we used the method as a learning tool to test, and more important, to reject hypotheses. In such a top-down approach, stepwise improvement of the model should be coupled with expert knowledge. Since a large amount of different observations are needed to constrain the different calibration parameters, all parameters and scenarios should be discussed for their physical meaning and realism (Seibert and McDonnell, 2002).

During the first discharge peak we calibrated 3 parameters: W_R, T_R and stream losses. In our case study W_R has limited physical meaning, since it corrects for errors in observed rainfall and discharge. The intensive rainstorm lasted for less than 10 min, while the logging interval of both, rainfall and discharge was also 10 min, which makes it likely that observed discharged is underestimated. Because the 'rain on water' and saturation overland flow is the main process causing the first discharge peak, a higher W_R could easily correct for these errors in the observations. Yet, the obtained value of 1.7 m seems realistic.

The temperature of the rain T_R is difficult to measure. As a first estimate air temperature was taken. However,the simulated in-stream temperature appeared to be too high during and just after the rainstorm, which was reason to decrease this temperature with 2.4 °C. This corresponds with the wet bulb temperature obtained with a relative humidity of 80%, which is similar to the observed relative humidity in Ettelbruck (ca. 6 km from the site).

Another result obtained is that infiltration losses are relative to in-stream discharge, while gains of water are constant over time. We can explain that with the fact that the whole catchment was relatively dry during the studied period and a 5 mm rainstorm is

HESSD
8, 2175–2205, 2011

not enough to increase the groundwater level or to initiate runoff from the hillslopes. Infiltration losses, on the other hand, can be large under these conditions and can vary with discharge. When the width of the stream increases, bank infiltration can increase. Due to the dry initial state, this infiltrated water can be retained in the stream bank after the water level decreases again.

From line *a* in Fig. 3 it is seen that when the infiltration loss between 60 and 77 m is taken constant over time, the peak in downstream discharge occurs 50 min too late. Therefore we can conclude with high certainty that this loss increases with increasing discharge. For the total amount of infiltration losses in this area, we assumed a linear relation between losses and discharge. However, numerous other relations or hysteretic loops may describe the infiltration loss better.

The variability of the infiltration loss between 233 and 247 m is less accurate. Assuming a constant loss here, would result in a downstream discharge peak lasting 15–20 min longer than observed (thus making the peak wider). Although a variable loss of 45% of upstream discharge gave better results, the difference between a constant and variable loss are much smaller than for the infiltration loss between 60 and 77 m.

Different hyporheic exchange scenarios were only tested during the second discharge peak. Reason for this is that during the first discharge peak, the different scenarios did not lead to significantly different temperatures. This could be caused by the fact that the discharge peak was not long enough to influence the temperature in the hyporheic zone significantly. The different scenarios during the second peak indicate that between 0 and 250 m Q_{hyp} and V_{hz} are variable with varying discharge, while downstream of 250 m they remain constant with varying discharge (Fig. 6a). A possible explanation for this spatial variability is that between 0 and 250 m, the width of the stream increases a lot during peak discharge: about 1.7 times during the second discharge peak and between 75 and 90 m the width increases to 6 to 10 times the original width, compared to a factor 1 to 1.3 for the area downstream of 250 m. This results in a much higher contact area between the stream and hyporheic zone. Beside the

HESSD
8, 2175–2205, 2011

increase in stream width, more upwelling groundwater could influence the hyporheic exchange as well (Harvey and Bencala, 1993; Harvey et al., 1996). However, as stated before, the catchment was dry, so in our case an increase in upwelling groundwater was most likely not the case.

The main objective of this study is to see where and when discharge was generated. Here we tested 3 hypotheses about the location of the missing water to close the water balance. The tested locations were chosen after the first results of the reference simulation of the second peak. In principle, each location could be tested, but with knowledge of the field site, only 3 locations where considered feasible. The location of the diffuse source (250–350 m) was chosen, since it directly influences the in-stream temperature at this location. However, the catchment was relatively dry, making it not so likely that a new source arises after such a small rainstorm and for such a short time. The hypothesis of the new source at 178 m, at the location of an already existing source would pass the realism check, since only some extra water is needed to increase the lateral inflow. However, our model results (especially expressed in $RMSE_L$ and Fig. 7) give reasons to reject this hypothesis .

In the third scenario, we hypothesize that a bypass becomes active during the second discharge peak. An active bypass has been observed during higher flows, and therefore it is likely that it happened during this event as well. It also means that a significant amount of water that we accounted for as infiltration loss between 60 and 77 m, filled the dry bypass, and only when the whole bypass was saturated, it connected to the stream again. The initial wetting up of the bypass would also explain the time lag between the first discharge peak and the activation of the bypass. Overall, the third scenario seems the most likely one, alhough the first scenario of a diffuse source between 250 and 350 m cannot be fully rejected either.

5.2 Limitation of method

Because temperature is used as a natural tracer, sufficient temperature fluctuations, both in space and time, are needed to be able to distinguish between different fluxes.

HESSD
8, 2175–2205, 2011

Unfortunately, we therefore could only apply this method during low flow and warm days as we use natural heating via solar input. During winter, we observed too small temperature fluctuations to apply this method. Even during larger summer rainstorms, the spatial and temporal temperature fluctuations were not large enough to differentiate between different runoff fluxes. We have to conclude that during high water conditions, when subsurface storm flow becomes active and hydrologically it becomes more interesting, the method cannot rely on solar energy input anymore, but sufficient additional energy has to be added to the stream.

Another interesting question was what would happen with the hyporheic exchange during non-steady state discharge conditions. The relation between hyporheic exchange and discharge or cross-sectional area is not known a priori. For reasons of simplicity, we only tested the linear relation between Q_{hyp} and cross-sectional area as described by Runkel (1998), versus no relation at all, while V_{hz} was assumed to be linearly dependent with the wetted perimeter. Although these relationships are arbitrary, it gives a first estimate of how hyporheic exchange varies with discharge.

In our case study the spatial and temporal distribution of both, hyporheic exchange and discharge had to be taken into account. In streams with limited hyporheic exchange, it is possible to focus only on the discharge distribution, making the method more reliable. The same is true when limited gains and losses are present in a stream. In such a case it may be possible to test more complex relations between hyporheic exchange and discharge.

6 Conclusions

In this paper we demonstrate a new method to identify spatial and temporal dynamics of in-stream discharge. We combined a routing model with an advection-dispersion model and an energy balance model, which we confronted with both, discharge observations and high resolution temperature observations. This model was calibrated for steady

HESSD
8, 2175–2205, 2011

state discharge by Westhoff et al. (2011). During this study, it has been used to unravel discharge dynamics during a small but intensive summer rainstorm.

Due to the complexity in this small stream, we used the model as a learning tool, where hypotheses were formulated, tested and rejected or accepted. We showed that during this rainstorm gains of water remained constant for the whole simulation period, while losses of stream water increase with increasing discharge. This resulted in large dampening of the observed upstream peak discharge, while "rain on water" and saturation overland flow in the riparian zone were the main processes responsible for the first discharge peak. During the second discharge peak, we simulated a too low downstream discharge, after which we tested different hypotheses on where the additional water came from. We conclude that most likely a bypass becomes active, which first had to be filled, before it was connected to the stream again.

Hyporheic exchange is likely to be variable with discharge in the upstream half of the stream, where the stream width increases significantly with increasing discharge, while in the downstream half temperature was better simulated if a constant hyporheic exchange was assumed.

Overall, the proposed method offers more detailed insight in spatial and temporal discharge dynamics, but for now application of this method is limited, because large amount of energy input is needed to create enough temperature differences in both space and time. In our case, we used only natural temperature variations, which made this method only applicable for a small intensive summer rainstorm, during low initial discharge. To apply this method during higher discharge or less favorable meteorological circumstances, more (artificial) energy input is needed. A possible way forward may be to test this method downstream of a large dam or reservoir.

Acknowledgements. We would like to thank Guus Stelling for his help with implementing the numerical schemes and the municipality of Ettelbruck for their cooperation. This research is partly funded by the Delft Cluster project Veiligheid tegen overstromingen: CT04.30.

HESSD
8, 2175–2205, 2011

References

Bartolino, J.: The Rio Grande – Competing demands for a desert river, Heat as a Tool for Studying the Movement of Ground Water Near Streams, edited by: Stonestrom, D. A. and Constantz, J., 8–16, 2003. 2178

Becker, M. W., Georgian, T., Ambrose, H., Siniscalchi, J., and Fredrick, K.: Estimating flow and flux of ground water discharge using water temperature and velocity, J. Hydrol., 296, 221–233, doi:10.1016/j.jhydrol.2004.03.025, 2004. 2177

Blasch, K., Constantz, J., and Stonestrom, D. A.: Thermal methods for investigation groundwater recharge, US Geological Survey Professional Paper, 1703, 353–376, 2007. 2178

Boano, F., Revelli, R., and Ridolfi, L.: Bedform-induced hyporheic exchange with unsteady flows, Adv. Water Resour., 30, 148–156, 2007. 2178

Bonell, M.: Selected challenges in runoff generation research in forests from the hillslope to headwater drainage basin scale, J. Am. Water Resour. As., 34, 765–785, doi:10.1111/j.1752-1688.1998.tb01514.x, 1998. 2176

Constantz, J.: Interaction Between Stream Temperature, Streamflow, and Groundwater Exchanges in Alpine Streams, Water Resour. Res., 34, 1609–1615, 1998. 2177

Constantz, J. and Thomas, C. L.: The Use of Streambed Temperature Profiles to Estimate the Depth, Duration, and Rate of Percolation Beneath Arroyos, Water Resour. Res., 32, 3597–3602, 1996. 2177

Constantz, J., Cox, M. H., Sarma, L., and Mendez, G.: The Santa Clara River – The last natural river of Los Angeles, Heat as a Tool for Studying the Movement of Ground Water Near Streams, edited by: Stonestrom, D. A. and Constantz, J., USGS Circular, 1260, 21–27, 2003. 2177

D'angelo, D., Webster, J., Gregory, S., and Meyer, J.: Transient storage in Appalachian and Cascade mountain streams as related to hydraulic characteristics, J. N. Am. Benthol. Soc., 223–235, 1993. 2178

Fenicia, F., McDonnell, J. J., and Savenije, H. H. G.: Learning from model improvement: On the contribution of complementary data to process understanding, Water Resour. Res., 44, W06419, 10.1029/2007WR006386, 2008. 2183

Gomi, T., Sidle, R. C., Miyata, S., Kosugi, K., and Onda, Y.: Dynamic runoff connectivity of overland flow on steep forested hillslopes: Scale effects and runoff transfer, Water Resour. Res., 44, W08411, 10.1029/2007WR005894, 2008. 2177

HESSD
8, 2175–2205, 2011

Ha, K., Koh, D., Yum, B., and Lee, K.: Estimation of river stage effect on groundwater level, discharge, and bank storage and its field application, Geosci. J., 12, 191–204, 2008. 2178
Habel, F. and Bagtzoglou, A.: Wave induced flow and transport in sediment beds, Journal of the American Water Resources Association, 41, 461–476, 2005. 2178
Hart, D., Mulholland, P., Marzolf, E., DeAngelis, D., and Hendricks, S.: Relationships between hydraulic parameters in a small stream under varying flow and seasonal conditions, Hydrol. Process., 13, 1497–1510, 1999. 2178
Harvey, J. and Bencala, K.: The effect of streambed topography on surface-subsurface water exchange in mountain catchments, Water Resour. Res., 29, 89–98, 1993. 2178, 2191
Harvey, J., Wagner, B., and Bencala, K.: Evaluating the reliability of the stream tracer approach to characterize stream-subsurface water exchange, Water Resour. Res., 32, 2441–2451, doi:10.1029/96WR01268, 1996. 2178, 2191
Harvey, J., Conklin, M., and Koelsch, R.: Predicting changes in hydrologic retention in an evolving semi-arid alluvial stream, Adv. Water Resour., 26, 939–950, 2003. 2178
Jothityangkoon, C., Sivapalan, M., and Farmer, D. L.: Process controls of water balance variability in a large semi-arid catchment: downward approach to hydrological model development, J. Hydrol., 254, 174–198, doi:10.1016/S0022-1694(01)00496-6, 2001. 2183
Klemeš, V.: Conceptualization and scale in hydrology, J. Hydrol., 65, 1–23, doi:10.1016/0022-1694(83)90208-1, 1983. 2183
Lal, A.: Modification of canal flow due to stream-aquifer interaction, J. Hydraul. Eng.g, 127, 567–576, 2001. 2178
Lapham, W. W.: Use of temperature profiles beneath streams to determine rates of vertical ground-water flow and vertical hydraulic conductivity, Available from Books and Open Files Report Section USGS Box 25425, Denver, CO 80225. USGS Water-Supply Paper 2337., 1989. 2177
Legrand-Marcq, C. and Laudelout, H.: Longitudinal dispersion in a forest stream, J. Hydrol., 78, 317–324, 1985. 2178
Monteith, J. L.: Evaporation and surface temperature, Q. J. Roy. Meteor. Soc., 107, 1–27, 1981. 2182
Morrice, J., Valett, H., Dahm, C., and Campana, M.: Alluvial characteristics, groundwater-surface water exchange and hydrological retention in headwater streams, Hydrol. Process., 11, 253–267, 1997. 2178
Niswonger, R. G., Prudic, D. E., Pohll, G., and Constantz, J.: Incorporating seepage losses

HESSD
8, 2175–2205, 2011

into the unsteady streamflow equations for simulating intermittent flow along mountain front streams, Water Resour. Res., 41, W06006, 10.1029/2004WR003677, 2005. 2177
Ragan, R. M.: An experimental investigation of partial area contributions, proc Berne Symp, Int. Assoc. Sci. Hydrol. Publ., 1968. 2177
Retter, M., Kienzler, P., and Germann, P. F.: Vectors of subsurface stormflow in a layered hillslope during runoff initiation, Hydrol. Earth Syst. Sci., 10, 309–320, doi:10.5194/hess-10-309-2006, 2006. 2177
Runkel, R. L.: One-dimensional transport with inflow and storage (OTIS): A solute transport model for streams and rivers, US Geological Survey Water-Resources Investigation Report, 98, 4018, 1998. 2185, 2192
Schmid, B. H.: Can Longitudinal Solute Transport Parameters Be Transferred to Different Flow Rates?, Journal of Hydrologic Engineering, 13, 505–509, doi:10.1061/(ASCE)1084-0699(2008)13:6(505), 2008. 2178
Schmid, B. H., Innocenti, I., and Sanfilippo, U.: Characterizing solute transport with transient storage across a range of flow rates: The evidence of repeated tracer experiments in Austrian and Italian streams, Adv. Water Resour., 33, 1340–1346, doi:10.1016/j.advwatres.2010.06.001, 2010. 2178
Seibert, J. and McDonnell, J. J.: On the dialog between experimentalist and modeler in catchment hydrology: Use of soft data for multicriteria model calibration, Water Resour. Res., 38, 1241, doi:10.1029/2001WR000978, 2002. 2189
Selker, J., van de Giesen, N., Westhoff, M., Luxemburg, W., and Parlange, M. B.: Fiber optics opens window on stream dynamics, Geophys. Res. Lett., 33, L24401, doi:10.1029/2006GL027979, 2006a. 2180
Selker, J. S., Thvenaz, L., Huwald, H., Mallet, A., Luxemburg, W., van de Giesen, N., Stejskal, M., Zeman, J., Westhoff, M., and Parlange, M. B.: Distributed fiber-optic temperature sensing for hydrologic systems, Water Resour. Res., 42, W12202, doi:10.1029/2006WR005326, 2006b. 2180
Silliman, S. E., Ramirez, J., and McCabe, R. L.: Quantifying downflow through creek sediments using temperature time series: one-dimensional solution incorporating measured surface temperature, J. Hydrol., 167, 99–119, doi:10.1016/0022-1694(94)02613-G, 1995. 2177
Sivapalan, M., Blschl, G., Zhang, L., and Vertessy, R.: Downward approach to hydrological prediction, Hydrol. Process., 17, 2101–2111, 2003. 2183
Sklash, M. G. and Farvolden, R. N.: The role of groundwater in storm runoff, J. Hydrol., 43,

HESSD
8, 2175–2205, 2011

45–65, doi:10.1016/0022-1694(79)90164-1, 1979. 2177
Stallman, R. W.: Steady one-dimensional fluid flow in a semi-infinite porous medium with sinusoidal surface temperature, J. Geophys. Res., 70, 2821–2827, 1965. 2177
Stelling, G. S. and Duinmeijer, S. P. A.: A staggered conservative scheme for every Froude number in rapidly varied shallow water flows, Int. J. Numer. Meth. Fl., 43, 1329–1354, 2003. 2181
Taniguchi, M. and Sharma, M. L.: Solute and heat transport experiments for estimating recharge rate, Journal of Hydrology, 119, 57–69, doi:10.1016/0022-1694(90)90034-U, 1990. 2177
Tromp-van Meerveld, H. J. and McDonnell, J. J.: Threshold relations in subsurface stormflow: 1. A 147-storm analysis of the Panola hillslope, Water Resour. Res., 42, W02410, doi:10.1029/2004WR003778, 2006. 2177
Tromp-van Meerveld, H. J., James, A. L., McDonnell, J. J., and Peters, N. E.: A reference data set of hillslope rainfall-runoff response, Panola Mountain Research Watershed, United States, Water Resour. Res., 44, W06502, doi:10.1029/2007WR006299, 2008. 2177
Tyler, S. W., Selker, J. S., Hausner, M. B., Hatch, C. E., Torgersen, T., Thodal, C. E., and Schladow, S. G.: Environmental temperature sensing using Raman spectra DTS fiber-optic methods, Water Resour. Res., 45, W00D23, doi:10.1029/2008WR007052, 2009. 2180
Uchida, T., Tromp-van Meerveld, I., and McDonnell, J. J.: The role of lateral pipe flow in hillslope runoff response: an intercomparison of non-linear hillslope response, J. Hydrol., 311, 117–133, doi:10.1016/j.jhydrol.2005.01.012, 2005. 2177
Uhlenbrook, S. and Hoeg, S.: Quantifying uncertainties in tracer-based hydrograph separations: a case study for two-, three- and five-component hydrograph separations in a mountainous catchment, Hydrol. Process., 17, 431–453, doi:10.1002/hyp.1134, http://dx.doi.org/10.1002/hyp.1134, 2003. 2177
Weiler, M., Naef, F., and Leibundgut, C.: Study of runoff generation on hillslopes using tracer experiments and a physically-based numerical hillslope model, IAHS Publications-Series of Proceedings and Reports-International Association of Hydrological Sciences, 248, 353–362, 1998. 2177
Westhoff, M. C., Savenije, H. H. G., Luxemburg, W. M. J ., Stelling, G. S., van de Giesen, N. C., Selker, J. S., Pfister, L., and Uhlenbrook, S.: A distributed stream temperature model using high resolution temperature observations, Hydrol. Earth Syst. Sci., 11, 1469–1480, doi:10.5194/hess-11-1469-2007, 2007. 2181, 2182

HESSD
8, 2175–2205, 2011

Westhoff, M. C., Bogaard, T. A., and Savenije, H. H. G.: Quantifying the effect of in-stream rock clasts on the retardation of heat along a stream, Adv. Water Resour., 33, 1417–1425, doi:10.1016/j.advwatres.2010.02.006, 2010. 2181

Westhoff, M. C., Gooseff, M. N., Bogaard, T. A., and Savenije, H. H. G.: Quantifying hyporheic exchange at high spatial resolution using natural temperature variations along a first order stream, Water Resour. Res., submitted, 2011. 2178, 2180, 2181, 2182, 2183, 2186, 2193

Woods, R. and Rowe, L.: The changing spatial variability of subsurface flow across a hillside, J. Hydrol., New Zealand, 35, 51–86, 1996. 2177

Wroblicky, G., Campana, M., Valett, H., and Dahm, C.: Seasonal variation in surface-subsurface water exchange and lateral hyporheic area of two stream-aquifer systems, Water Resour. Res., 34, 317–328, 1998. 2178

Zarnetske, J. P., Gooseff, M. N., Brosten, T. R., Bradford, J. H., McNamara, J. P., and Bowden, W. B.: Transient storage as a function of geomorphology, discharge, and permafrost active layer conditions in Arctic tundra streams, Water Resour. Res., 43, W07410, doi:10.1029/2005WR004816, 2007. 2178

HESSD
8, 2175–2205, 2011

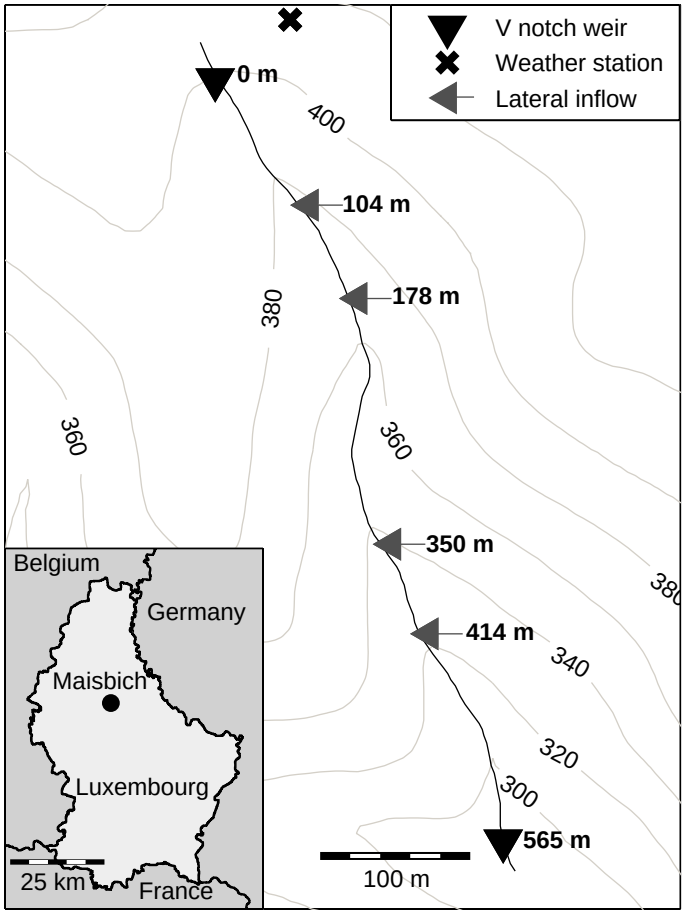

Fig. 1. Map of the studied stretch of the Maisbich. The isohypse show the altitude above mean sea level. Distances of the lateral inflows are distances from the upstream V-noth weir measured along the stream.

HESSD
8, 2175–2205, 2011

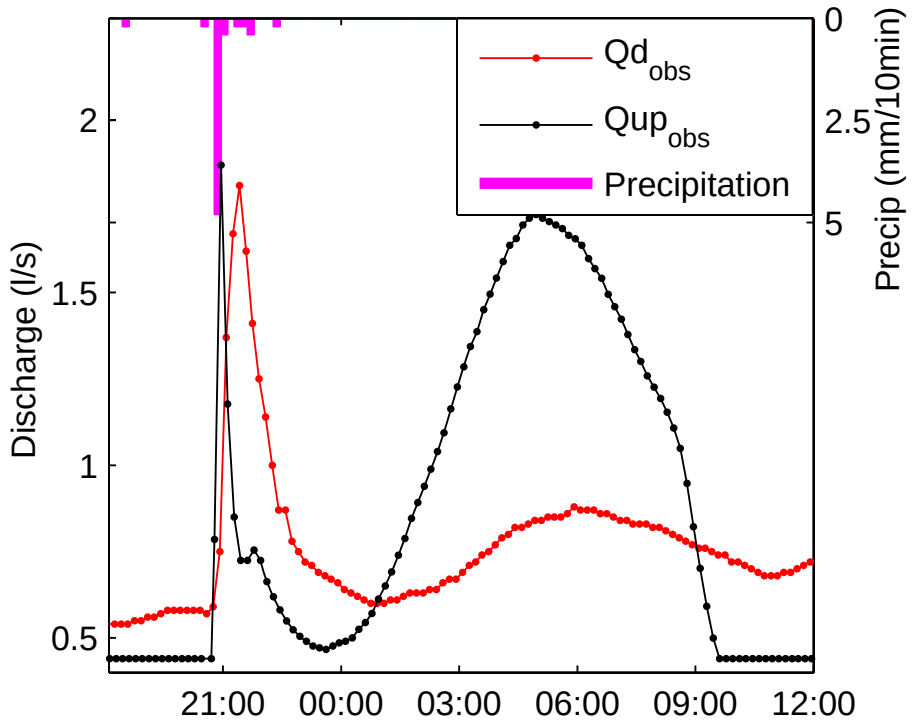

Fig. 2. Observed upstream (Qup_{obs}) and downstream (Qd_{obs}) discharge during the event of 22 and 23 June 2008. Note that before 20:40 and after 10:00 h, the noise in upstream discharge observations was removed to decrease calculation time.

HESSD
8, 2175–2205, 2011

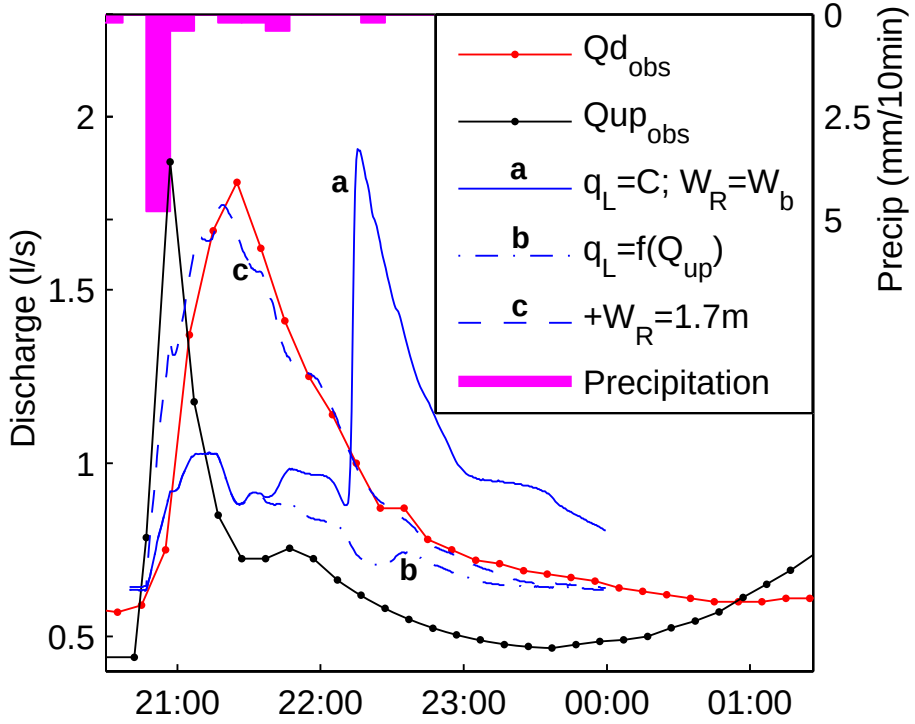

Fig. 3. Observed and simulated first discharge peak on 22 June 2008. The subscripts d and up refer to downstream and upstream.

HESSD
8, 2175–2205, 2011

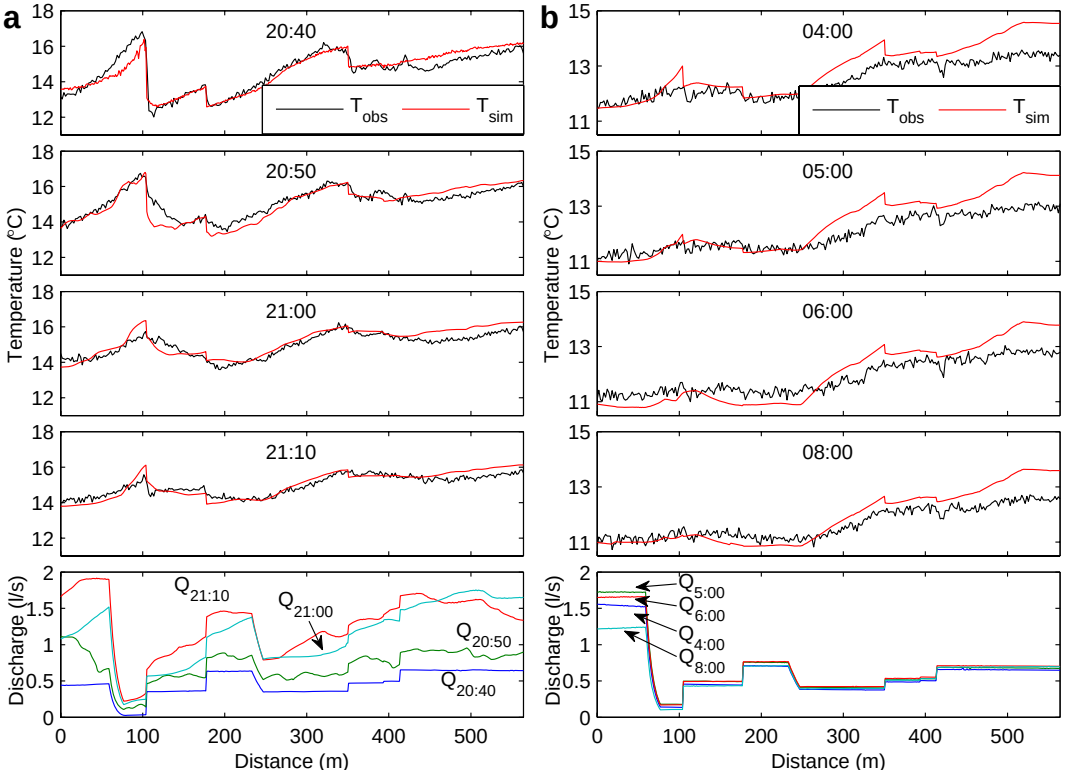

Fig. 4. Observed and simulated temperature and simulated discharge during **(a)** first discharge peak (after calibration) and **(b)** second discharge peak using the same parameters as during the first discharge peak. Q_{hyp} and V_{hz} are variable over time.

HESSD
8, 2175–2205, 2011

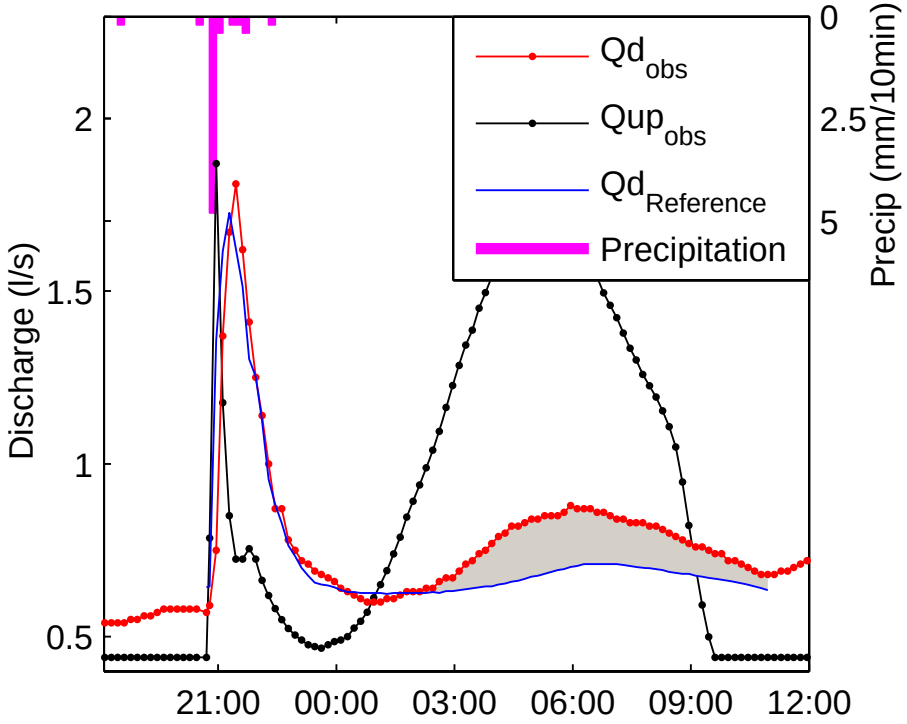

Fig. 5. Observed and simulated discharge of second peak on 22 and 23 June 2008, using the same parameters as during the first discharge peak. The shaded area is the difference between observed and simulated discharge.

HESSD
8, 2175–2205, 2011

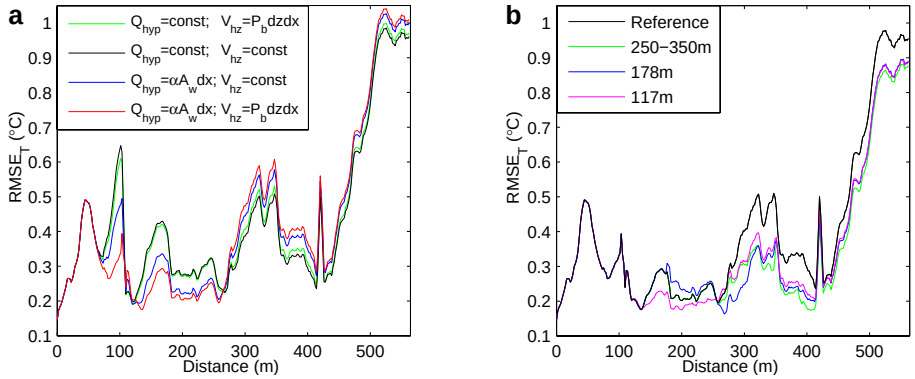

Fig. 6. $RMSE_T$ for **(a)** different hyporheic exchange scenarios, and **(b)** different locations of the new source. Reference refers to the simulation where Q_{hyp} and V_{hz} are variable between 0 and 250 m and constant between 250 and 564 m, but without the new source. The numbers of the other solutions are the location of the new source. A moving average of 3 observation point in space was taken for all time series between 23 June 2008 01:00 and 10:00 h.

HESSD
8, 2175–2205, 2011

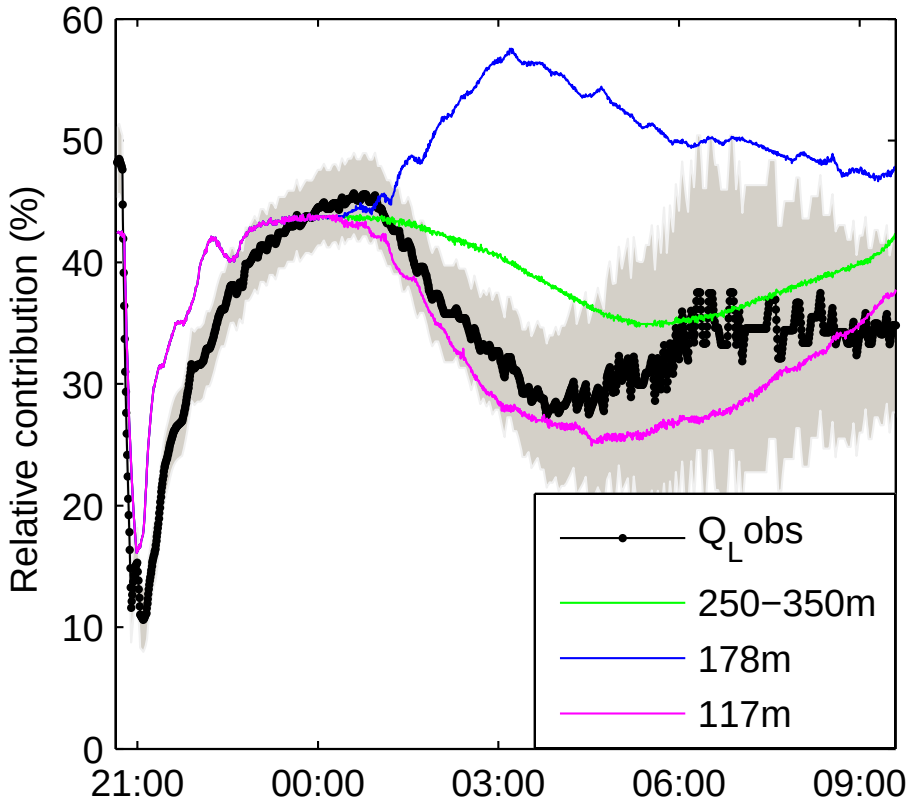

Fig. 7. Observed and simulated (3 scenarios) relative contribution of the second source. The different scenarios are the locations where the new source was added. Shaded area is observed contribution $\pm 1\sigma$.

HESSD
8, 2175–2205, 2011